

The Application of Chirp Z-Transform in Fast Computation of Antenna Array Pattern

Cheng Zhang¹, Anyong Qing^{2,1}, and Yang Meng¹

¹ School of Physics

University of Electronic Science and Technology of China, Chengdu, 610054, China
zhangcheng_uestc@163.com, mengy.1003@163.com

² School of Electrical Engineering

Southwest Jiaotong University, Chengdu, 610031, China
qinganyong@tsinghua.org.cn

Abstract — As an essential means of evaluating antenna array performance and the basis of antenna array design, numerical computation of antenna array pattern is very important. Computation of antenna array pattern by using straightforward summation is very time consuming especially for planar array with many elements. Moreover, in some applications such as antenna array synthesis, huge number of repeated pattern computations is needed that the consumed time is intolerably long. Although the computation can be accelerated by fast Fourier transform (FFT) when the elements are equally spaced by half of a wavelength because the array factor and the element excitation currents is a Fourier transform pair, in general, FFT is not applicable. In this paper, the chirp z-transform (CZT) is introduced to accurately and efficiently compute pattern of general linear or planar antenna arrays. Numerical examples confirm that CZT is flexible, efficient, and accurate.

Index Terms — Antenna array pattern, chirp z-transform, FFT, linear antenna array, planar antenna array.

I. INTRODUCTION

Usually antenna arrays instead of bulky single-element antennas are deployed for higher directivity, narrower beam width, anti-interference ability and so on. Numerical computation of antenna array pattern is very important because it is an essential means of evaluating antenna array performance and is the basis of antenna array design [1].

In practice, array elements are often but not necessarily identical for convenience and simplicity. In this case, the array pattern of an ideal array is usually represented by its array factor.

For the general linear antenna array with N elements as shown in Fig. 1, its array factor reads:

$$AF(u, u_0) = \sum_{n=1}^{N-1} I_n \cdot \exp\left[j2\pi \frac{x_n}{\lambda}(u - u_0)\right], \quad (1)$$

where $u = \cos\theta$, $\theta \in [0, \pi]$, $u_0 = \cos\theta_0$, θ_0 is the desired beam steering direction, I_n and x_n are the excitation current and the position of the n th element, respectively, λ is the wavelength.

For the general planar antenna array with N elements as shown in Fig. 2, its array factor is given by:

$$AF(u, v, u_0, v_0) = \sum_{n=0}^{N-1} I_n \cdot \exp\left[jx_n \frac{2\pi}{\lambda}(u - u_0) + jy_n \frac{2\pi}{\lambda}(v - v_0)\right], \quad (2)$$

where u and v are defined in terms of sine space coordinates $u = \sin\theta\cos\phi$ and $v = \sin\theta\sin\phi$, $u_0 = \sin\theta_0\cos\phi_0$, $v_0 = \sin\theta_0\sin\phi_0$, (θ_0, ϕ_0) is the main beam steering direction, I_n and (x_n, y_n) are the excitation current and the position of the n th element, respectively.

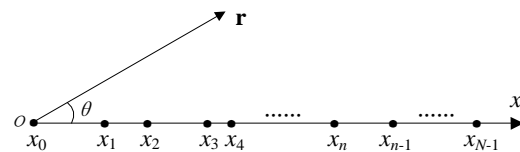


Fig. 1. General linear antenna array.

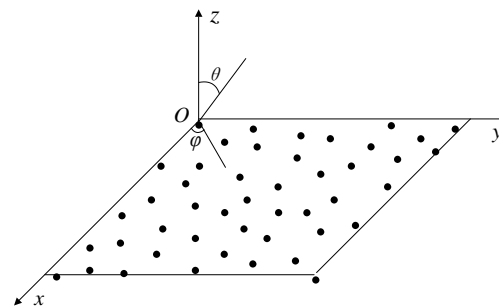


Fig. 2. General planar antenna array.

In some applications such as phased antenna array synthesis, the number of computations of array factor T might be extremely high. In general, T reads:

$$T = a \cdot b \cdot c, \quad (3)$$

where a is the number of directions for a fixed array at fixed main beam direction. To evaluate the array performance, the array factor has to be calculated at as many directions as possible within a given range. b is the number of scanning angles (u_0, v_0) of interest. Different patterns might be required when the main beam scanning at different scanning angles. c is the number of antenna arrays considered during the complete synthesis process. Thousands or even more antenna arrays with fixed main beam direction and different weights need to be evaluated when optimizing array excitations by using methods such as statistical strategy optimization techniques [2-4].

For the planar antenna array considered in section 3C, calculation of array factor with $a=512 \times 512$ directions by using the brute-force method (BFM) will be taken about 15.2 seconds. If $b=100$ scanning angles (u_0, v_0) are considered and $c=10000$ times of array factor calculations for each scanning angle are needed, thus $T \approx 2.62 \times 10^{11}$. The corresponding consumed time is about 1.52×10^7 and it is intolerably long. Therefore, fast computation of array factor is utmost importance.

For an array with equally spaced elements, the array factor and the element excitation currents are a Fourier transform pair as expressed in (4). The formal expression of inverse discrete Fourier transform (IDFT) is also given in (5):

$$AF(u_k) = \sum_{n=-(N-1)/2}^{(N-1)/2-1} I_n \cdot e^{j2\pi n \frac{d}{\lambda} u_k}, k = -\frac{K-1}{2}, \dots, \frac{K-1}{2} - 1, \quad (4)$$

$$x(n) = \sum_{k=-(N-1)/2}^{(N-1)/2-1} \frac{X(k)}{N} e^{j2\pi k \frac{n}{N}}, n = -\frac{(N-1)}{2}, \dots, \frac{(N-1)}{2} - 1. \quad (5)$$

It might be a feasible way by adopting fast Fourier transform (FFT) in order to accelerate the computation of array factor [5]. However, compared (4) and (5), it can be seen that one of the correspondences holds:

$$\frac{n}{N} \longleftrightarrow \frac{d}{\lambda} u_k. \quad (6)$$

Expression (5) can be re-written as:

$$\frac{n}{N} \cdot \frac{\lambda}{d} \longleftrightarrow u_k. \quad (7)$$

Due to $-0.5 \leq n/N \leq 0.5$ and $-1 \leq u_k \leq 1$, the condition $\lambda/d=2$ must be met. In other words, FFT can be directly used to compute pattern of array with elements spacing only equal to half of wavelength depicted in Fig. 3. For general arrays, FFT cannot be directly applied.

In this paper, a versatile, efficient, and accurate approach to compute patterns of general antenna arrays with arbitrary spacing between array elements is proposed. The novel approach is based on CZT [6-7] which provides greater flexibility compared to FFT

for calculation of array factor. The corresponding parameters of CZT for antenna array factor computation are derived. Computation processes are also explored and given in this paper. Simulation results prove that it is applicable with high accuracy and efficiency, especially for planar array with equally or unequally spaced elements.

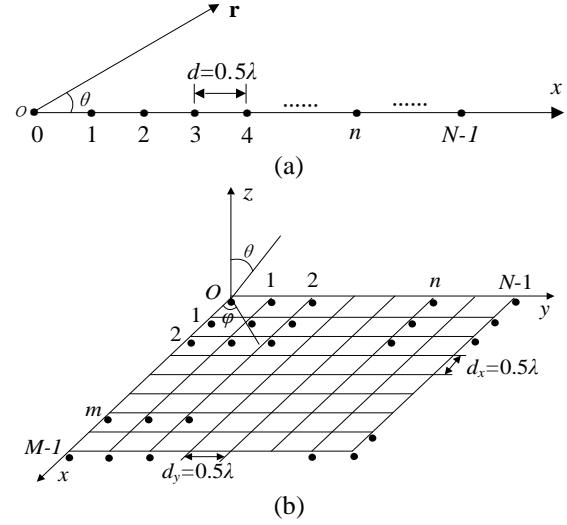


Fig. 3. Antenna arrays with elements spacing equal to half of a wavelength: (a) linear array and (b) planar array.

II. CHIRP Z-TRANSFORM FOR FAST COMPUTATION OF ARRAY FACTOR

A. One-dimension chirp z-transform

For an N -point sequence $x(n)$, CZT samples along spiral arcs in the z -plane as:

$$X(z_k) = \sum_{n=0}^{N-1} x(n) z_k^{-n}, \quad (8)$$

where $z_k = AW^k$, $k = 0, 1, \dots, K-1$, K is the number of points to calculate, A is the complex starting point, and W is the complex ratio between points.

In particular, if $A = A_0 e^{j2\pi\phi_0}$ and $W = e^{j2\pi\phi_0}$, CZT can be expressed as a convolution and computed efficiently by using Rabiner's algorithm [6].

B. Two-dimension chirp z-transform

2-D CZT of sequence $x(m, n)$ was derived by Draidi [7]:

$$X(z_{1k}, z_{2l}) = \sum_{m=0}^{M-1} \sum_{n=0}^{N-1} x(m, n) z_1^{-m} z_2^{-n}, \quad (9)$$

where $z_{1k} = A^1 W_1^{-k}$, $z_{2l} = A^2 W_2^{-l}$, $k = 0, \dots, K-1$, $l = 0, \dots, L-1$, $A^1 = A_0^1 e^{j2\pi\phi_{01}}$, $W_1 = e^{j2\pi\phi_{01}}$, $A^2 = A_0^2 e^{j2\pi\phi_{02}}$, and $W_2 = e^{j2\pi\phi_{02}}$.

The above 2-D CZT can be efficiently computed by using row-column decomposition and 1-D CZT.

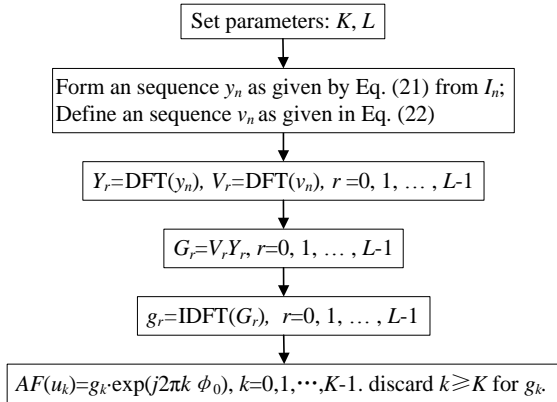


Fig. 4. The flow chart of pattern computation of linear array with equally spaced elements.

C. 1-D chirp z-transform for linear antenna array

For a linear antenna array with N equally spaced elements, (1) can be re-written as,

$$AF(u_k) = \sum_{n=0}^{N-1} I_n e^{j\psi_n u_k}, \quad (10)$$

where $u_k = \cos\theta_k$, $k=0, 1, \dots, K-1$, K is the total number of angles to sample, $0 \leq \theta_k \leq \pi$ is the k th sampled angle, $\psi_k = \beta d u_k - \psi_0$, $\beta = 2\pi/\lambda$ is the phase constant, d is the space between neighboring elements, $\psi_0 = \beta d u_0$ is the progressive phase delay between neighboring elements.

Let $z_k = e^{-j\psi_k}$, we have:

$$AF(u_k) = \sum_{n=0}^{N-1} I_n z_k^{-n}. \quad (11)$$

Obviously, CZT can be applied to compute the array factor $AF(u_k)$ efficiently if the following conditions are satisfied:

$$z_k = e^{-j(\beta d \cos\theta_k - \psi_0)} = A_0 e^{j2\pi\omega_0} e^{-jk2\pi\phi_0}. \quad (12)$$

Equivalently, we have:

$$A_0 = 1, \quad (13)$$

$$2\pi\omega_0 = \psi_0 - \beta d, \quad (14)$$

$$2\pi\omega_0 - (K-1)2\pi\phi_0 = \psi_0 + \beta d, \quad (15)$$

$$\beta d \cos\theta_k - \psi_0 = k2\pi\phi_0 - 2\pi\omega_0. \quad (16)$$

Therefore, the parameters of CZT for computation of $AF(u_k)$ are:

$$A_0 = 1, \quad (17)$$

$$\omega_0 = \frac{u_0 - 1}{2\pi} \beta d, \quad (18)$$

$$\phi_0 = -\frac{\beta d}{(K-1)\pi}, \quad (19)$$

$$\theta_k = \cos^{-1} \frac{K-1-2k}{K-1}. \quad (20)$$

After derivation of the parameters, the calculation

process addressed in [6] of CZT can be directly used to compute the linear array factor. A more detailed illustration is also given in this paper and shown in Fig. 4. In step 1, set L to be the smallest integer greater than or equal to $N+K-1$. The forms of y_n and v_n in step 2 are similar to the forms addressed in [6] and reads:

$$y_n = \begin{cases} I_n e^{-j2\pi n \omega_0} e^{j\pi n^2 \phi_0}, & 0 \leq n \leq N-1, \\ 0, & N \leq n \leq L-1 \end{cases}, \quad (21)$$

$$v_n = \begin{cases} e^{-j\pi n^2 \phi_0}, & 0 \leq n \leq K-1 \\ e^{-j\pi(L-n)^2 \phi_0}, & L-N+1 \leq n \leq L-1. \\ 0, & \text{other } n \end{cases}. \quad (22)$$

The convolution of y_n and v_n is the major part of the computational effort and requires a time roughly proportional to $(N+K) \log(N+K)$. It can be achieved by using DFT and the details are displayed in step 3~step 5 [8]. The DFT and inverse DFT (IDFT) can be accelerated by using FFT. Therefore, the computation speed is very fast.

In nature, the 1-D CZT imposes no limitation on element space d in regular linear array. It can be further extended to linear array with unequally spaced elements as shown in Fig. 5.

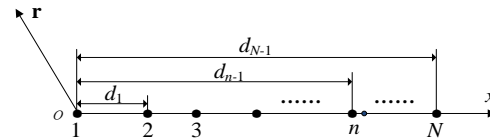


Fig. 5. A linear array with unequally spaced elements.

The extension works as follows:

1) Refine the linear array with N unequally spaced elements into a virtual one as shown in Fig. 6 with N_e equally spaced elements of space d_u , which is determined by the following expression:

$$d_u = \max \left[\min \sum_n \left\lceil \frac{d_n}{d_u} \right\rceil d_u - d_n \right], \quad (23)$$

where the symbol $\lfloor x \rfloor$ stands for the integer nearest to the real number x ;

2) Place the original elements to the nearest node in the virtual array without changing their excitations, and deactivate all element on other nodes by setting excitation currents $I_m = 0$;

3) Apply the 1-D CZT to compute the pattern.

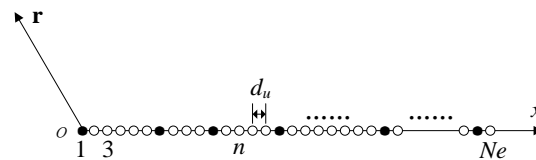


Fig. 6. The virtual linear array.

D. 2-D chirp z-transform for planar antenna array

For a planar antenna array with elements arranged in a rectangle grid at distance d_x and d_y along M rows and N column. (2) can be re-written as:

$$AF(u_{kl}, v_{kl}) = \sum_{m=0}^{M-1} \sum_{n=0}^{N-1} I_{mn} e^{j[m\beta d_x(u_{kl}-u_0)+n\beta d_y(v_{kl}-v_0)]}, \quad (24)$$

where $u_{kl}=\sin\theta_{kl}\cos\varphi_{kl}$ and $v_{kl}=\sin\theta_{kl}\sin\varphi_{kl}$, $k=0, \dots, K-1$, $l=0, \dots, L-1$.

By checking the analogy between (9) and (24), it is very clear that $AF(u_{kl}, v_{kl})$ can be more efficiently computed by applying 2-D CZT if its parameters are appropriately set. Derivation of parameters is similar to the 1-D CZT. Due to page limitation, the lengthy derivation process is omitted. The parameters are:

$$A_0^1 = A_0^2 = 1, \quad (25)$$

$$\phi_{01} = \frac{-\beta d_x}{(K-1)\pi}, \quad (26)$$

$$\phi_{02} = \frac{-\beta d_y}{(L-1)\pi}, \quad (27)$$

$$\omega_{01} = \frac{u_0-1}{2\pi} \beta d_x, \quad (28)$$

$$\omega_{02} = \frac{v_0-1}{2\pi} \beta d_y, \quad (29)$$

$$\theta_{kl} = \cos^{-1} \sqrt{\left(\frac{K-1-2k}{K-1}\right)^2 + \left(\frac{L-1-2l}{L-1}\right)^2}, \quad (30)$$

$$\varphi_{kl} = \sin^{-1} \frac{\frac{L-1-2l}{L-1}}{\sqrt{\left(\frac{K-1-2k}{K-1}\right)^2 + \left(\frac{L-1-2l}{L-1}\right)^2}}. \quad (31)$$

The flow chart of array factor computation of planar array with equally spaced elements is shown in Fig. 7.

In this paper, 2-D CZT is efficiently performed by using 1-D CZT with row-column decomposition [7]. In step 1, set P_1 to be the smallest integer greater than or equal to $M+K-1$, and set P_2 to be the smallest integer greater than or equal to $N+L-1$. In step 2, $v(p_1, p_2)$ is similar with $g(n, m)$ addressed in [7] and given in (32). The forms of $v(p_1, p_2)$ and $vh(p_1, p_2)$ are similar with the forms of v_n illustrated in (22) and given in (33)~(34), respectively:

$$h(p_1, p_2) = \begin{cases} I_{p_1 p_2} e^{j2\pi(p_1 a_{h1} + p_2 a_{h2})} e^{j\pi(\phi_{01} p_1^2 + \phi_{02} p_2^2)}, & \begin{cases} 0 \leq p_1 \leq M-1, \\ 0 \leq p_2 \leq N-1 \end{cases} \\ 0, & \text{other } p_1 \text{ and } p_2 \end{cases} \quad (32)$$

$$v(p_1, p_2) = \begin{cases} e^{-j\pi\phi_{02} p_2^2}, & 0 \leq p_1 \leq M-1, 0 \leq p_2 \leq L-1 \\ e^{-j\pi\phi_{01}(P_1-p_1)^2/2}, & \begin{cases} 0 \leq p_1 \leq M-1, \\ P_2-N+1 \leq p_2 \leq P_2-1 \end{cases} \\ 0, & \text{other } p_1 \text{ and } p_2 \end{cases} \quad (33)$$

$$vh(p_1, p_2) = \begin{cases} e^{-j\pi\phi_{01} p_1^2}, & 0 \leq p_1 \leq K-1, 0 \leq p_2 \leq P_2-1 \\ e^{-j\pi\phi_{01}(P_1-p_1)^2/2}, & \begin{cases} P_1-M+1 \leq p_1 \leq P_1-1, \\ 0 \leq p_2 \leq P_2-1 \end{cases} \\ 0, & \text{other } p_1 \text{ and } p_2 \end{cases} \quad (34)$$

In step 3~step 5, we first compute the CZT of each row of $h(p_1, p_2)$, put the result into an intermediate array, and then compute the CZT of each column of the intermediate array in step 7~step 9. Similarly, FFT is used to accelerate the DFT and IDFT. Therefore, the consumed time is substantially reduced.

It can be similarly generalized to efficiently compute array factors of planar arrays with unequally spaced elements, for example, triangular arrays whose elements are arranged in a triangular grid.

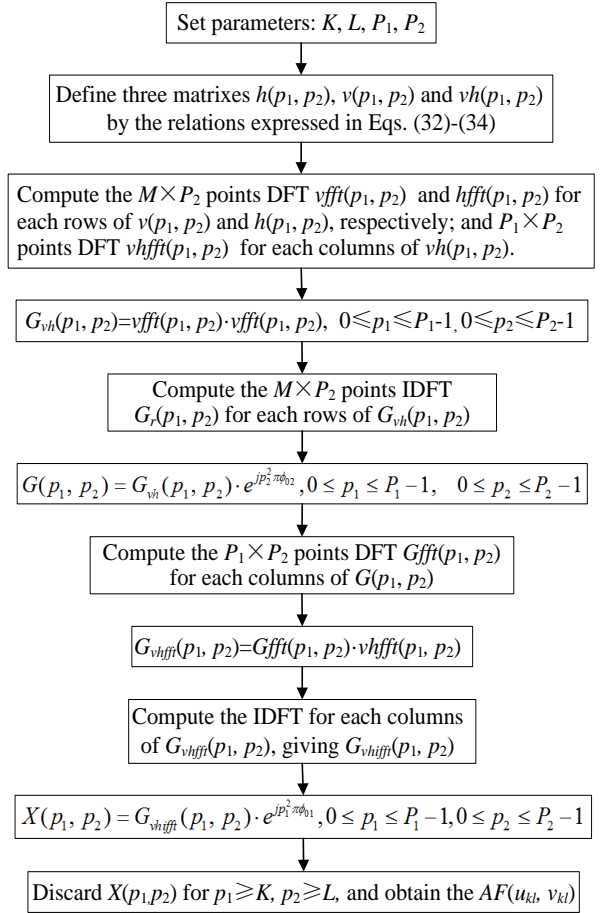


Fig. 7. The flow chart of array factor computation of planar array with equally spaced elements.

III. NUMERICAL RESULTS

A. Linear array with unequally spaced elements

The first linear array is one with 32 equally spaced elements of $d=0.7\lambda$. The excitations follow a Chebyshev

distribution [9] with $SLL=-35\text{dB}$ and $\theta_0=20^\circ$. The array factor computed by 1-D CZT is depicted in Fig. 8. Obviously, it agrees very well with that by BFM.

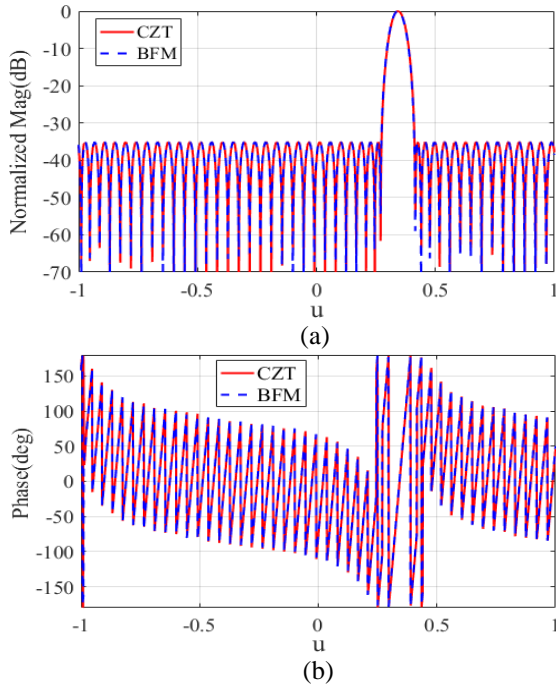


Fig. 8. Comparison of Chebyshev patterns computed by CZT and BFM: (a) magnitude and (b) phase.

The second linear array is a 40-element Woodward array [10] having a space $d=0.32\lambda$ and half beam width 20° . Once again, as shown in Fig. 9, the patterns by the two approaches overlap.

Figure 10 shows the time consumed by the two methods for computing linear array factors with various number of elements. It can be seen that the consumed time grows linearly with number of elements for both methods. The slope of CZT is 0.004×10^{-3} that its consumed time is almost constant for the studied number of elements. On the other hand, the slope of BFM is 0.05×10^{-3} that the consumed time difference becomes bigger and bigger as the number of elements increases beyond 30. Therefore, CZT is more suitable for large linear arrays with equally spaced elements.

B. Linear array with unequally spaced elements

A 37-element array with uniform excitation and unequally spaced elements addressed in Table 3 of [11] is re-visited here. Distribution of elements is extremely irregular that it is hardly possible to align all elements in the refined array with the corresponding elements in the actual array regardless of d_u . From the point of view of time consumption, the above observation in Section 3A of this paper hints that it is flexible to set as small as possible d_u for better alignment and consequently better

accuracy of the computed array factor by CZT. The effect of d_u on computational accuracy and computational time is shown in Table 1. The accuracy at $d_u=0.02\lambda$ is fairly good, as can be further demonstrated by the array factor in Fig. 11. Meanwhile, both actual computation time and its increment are negligibly small even if the virtual antenna array is 20 times denser.

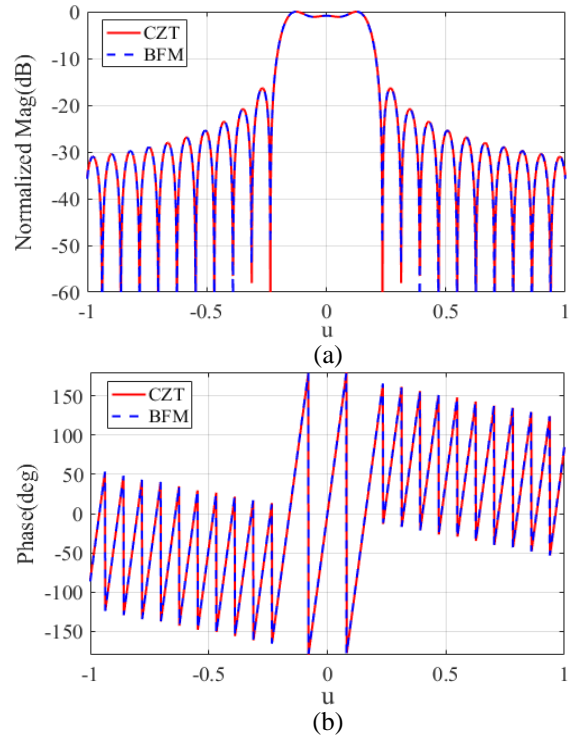


Fig. 9. Comparison of Woodward patterns computed by CZT and BFM: (a) magnitude, and (b) phase.

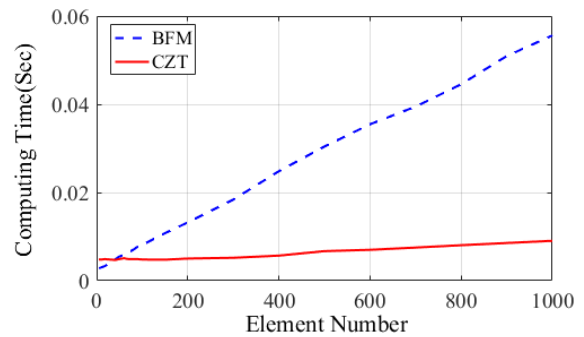


Fig. 10. Comparison of consumed time for computing array factors with equally spaced elements.

Table 1: Comparison of accuracy and consumed time

d_u	Mag. (dB)	Phase (Deg)	CZT (Sec)
0.005λ	0.1	1	0.031
0.01λ	0.19	1.5	0.022
0.05λ	0.45	4.5	0.014
0.1λ	1.1	12	0.013

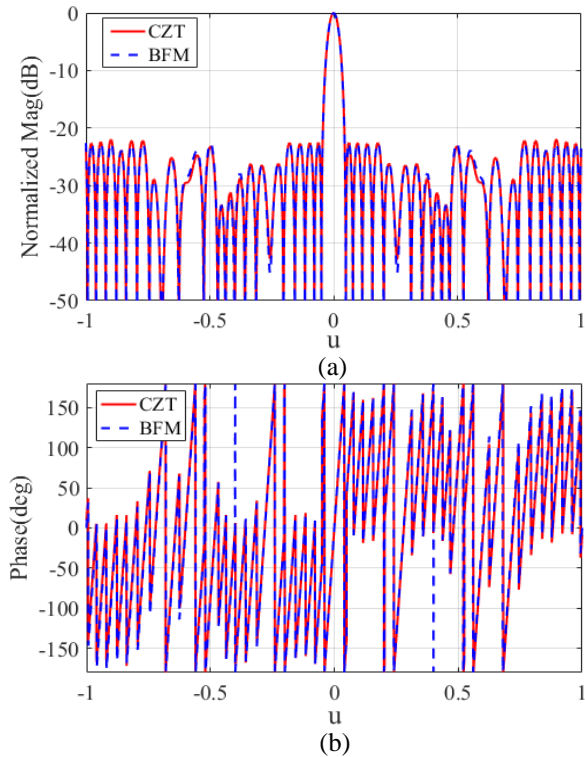


Fig. 11. Comparison of patterns of linear array with unequally spaced elements: (a) magnitude, and (b) phase.

C. Planar array with equally spaced elements

A rectangular planar array consisting of $M=24$ rows and $N=32$ columns of elements arranged along a rectangular grid with $d_x=0.7\lambda$ and $d_y=0.4\lambda$ is used to illustrate the capability of the 2-D CZT. Its main beam is pointed at $(\theta_0=20^\circ, \varphi_0=45^\circ)$ and a Chebyshev response is assumed to suppress the sidelobe at -35dB .

Figure 12 shows the magnitude and phase patterns computed by the 2-D CZT and BFM in the $u-v$ coordinates. The patterns computed by the two methods are almost identical. For clarity, the u -cuts of the patterns at $v=0.242$ is drawn in Fig. 13. The differences of $PSLL$ and phase are less than 0.2 dB and 3.5° .

The consumed time of the two methods for computing planar array factors with various numbers of equally spaced elements is shown in Fig. 14. The consumed time of 2-D CZT is almost constant. The consumed time is less than 0.15 second even for arrays with ten thousand elements. For BFM, the consumed time is about 176 second, which is 1173 times to 2-D CZT.

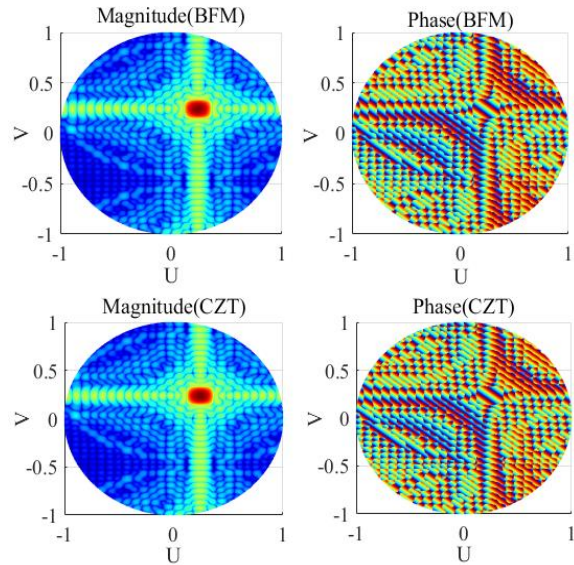


Fig. 12. Comparison of planar array patterns computed by BFM and CZT.

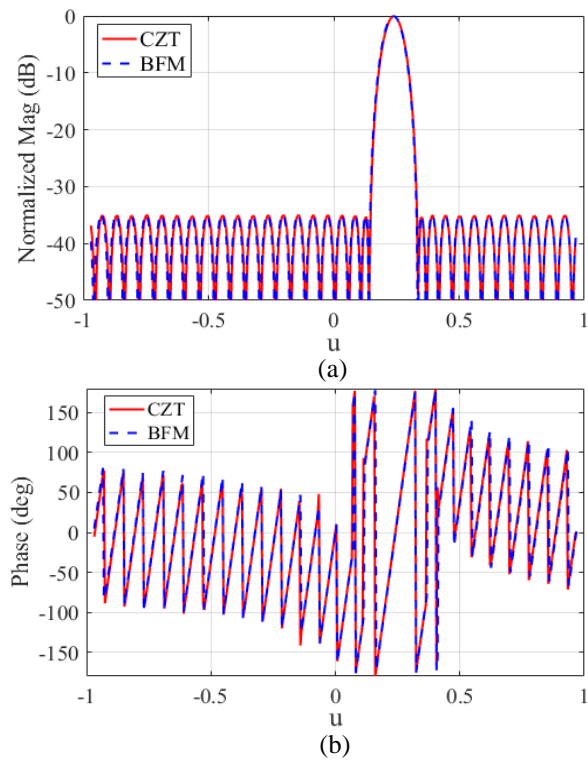


Fig. 13. u -cuts at $v=0.242$: (a) magnitude and (b) phase.

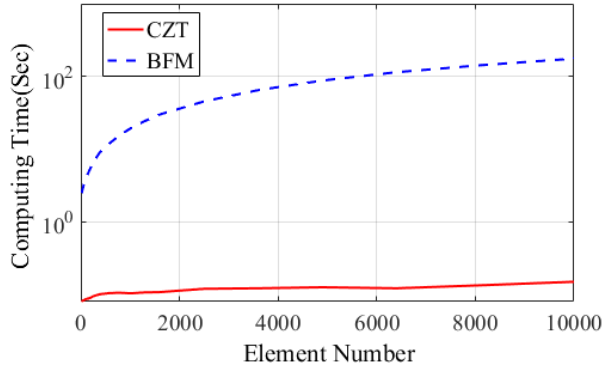


Fig. 14. Consumed time of CZT and BFM with various element numbers.

It is common sense that pattern of larger planar array has to be more finely sampled to reduce error. The consumed time with different number of sampling points of the above mentioned uniform planar array factor is listed in Table 2. Both grow as the number of sampling points increases. More importantly, the ratio between them becomes larger and larger. It can therefore be concluded that 2-D CZT is more advantageous to BFM in computing large planar array.

Table 2: Consumed time with different sampling points

Sampling Points	CZT (Sec)	BFM (Sec)
256×256	0.03	3.78
512×512	0.11	15.21
768×768	0.17	33.6
1024×1024	0.27	60.46
1536×1536	0.55	134.38

D. Planar array with unequally spaced elements

Figure 15 shows a planar phased antenna array with 576 unequally spaced elements. The array was illuminated by uniform excitation and its main beam is pointed at ($\theta_0=30^\circ$, $\varphi_0=60^\circ$).

Likewise, distribution of elements here is also extremely irregular that it is hardly possible to align all elements in the refined array with the corresponding elements in the actual array regardless of d_u and d_v . Fortunately, the above observation in section 3C of this paper allows us to flexibly set as small as possible d_u and d_v for better alignment and consequently better accuracy of the computed array factor by CZT. A similar study on the effect of d_u and d_v on computational accuracy is conducted. For simplicity, only cases of $d_u = d_v$ are investigated as shown in Table 3. The accuracy at $d_u = d_v = 0.02\lambda$ is fairly good while CZT always consumes much less time than BFM.

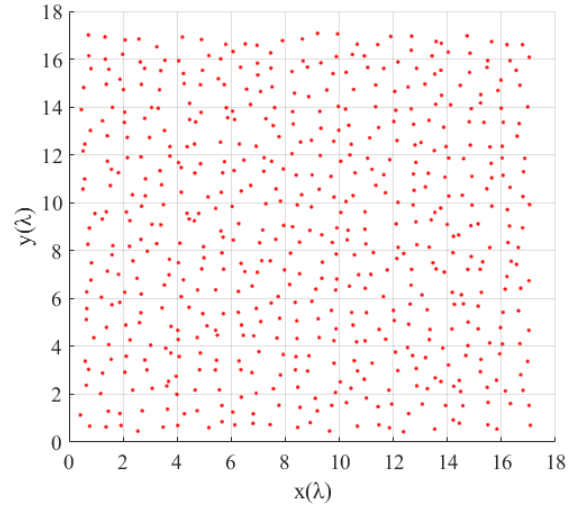


Fig. 15. A planar array with unequally spaced elements.

The actual array is accordingly refined $d_u = 0.02\lambda$ in x directions and $d_v = 0.02\lambda$ in y directions. The patterns computed by the two methods are shown in Fig. 16. For clarity, the u -cuts of the patterns at $v=0.25$ is drawn in Fig. 17. The $PSLL$ and phase differences are less than 0.05dB and 4.4° .

Table 3: Comparison of computational accuracy and computational time

d_u and d_v	Mag. (dB)	Phase (Deg)	2-D CZT	BFM (Sec)
0.01λ	0.03	2.5	2.78	12.55
0.02λ	0.05	4.4	1.21	12.55
0.05λ	0.05	6.8	0.54	12.55
0.1λ	0.06	9.5	0.33	12.55

Similarly, the consumed time with different number of sampling points of the above mentioned non-uniform planar array factor is listed in Table 4. The consumed time for both methods is proportional to the number of sampling points. More importantly, the ratio between them becomes larger and larger. It can therefore be concluded that 2-D CZT is more advantageous to BFM in computing large planar array.

Table 4: Comparison of consumed time with different sampling points

Sampling Points	2-D CZT	BFM (Sec)
256×256	0.88	2.97
512×512	1.21	12.55
768×768	1.85	27.99
1024×1024	2.35	50.66
1536×1536	3.57	108.04

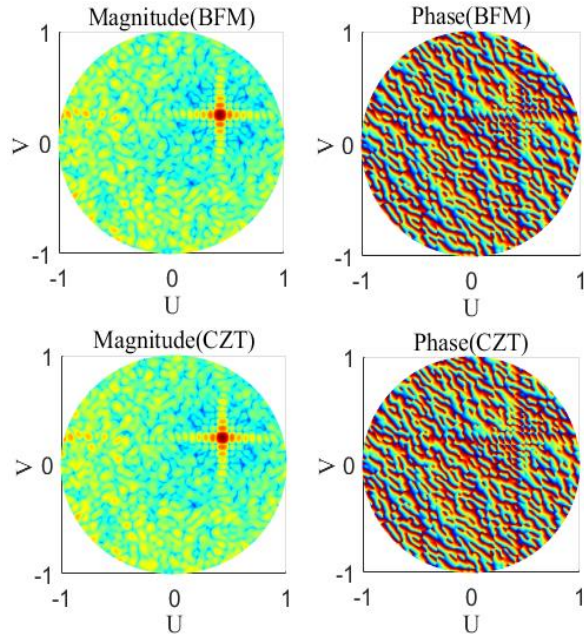


Fig. 16. Comparison of patterns computed by BFM and CZT, respectively.

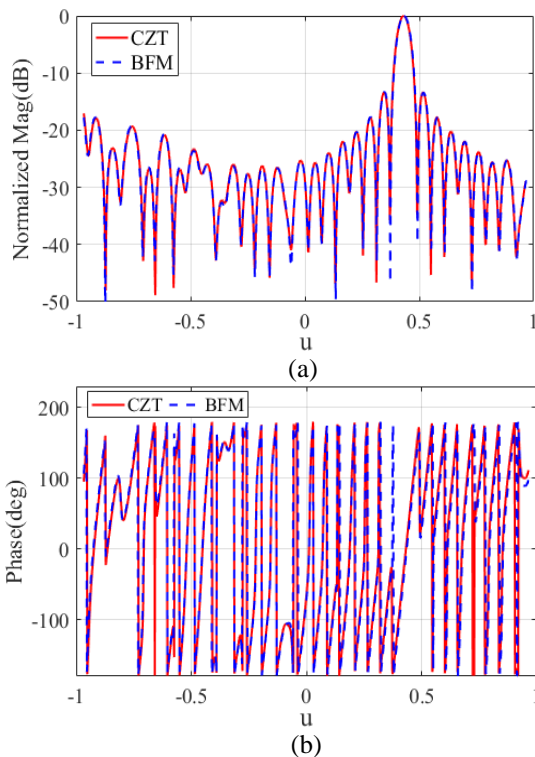


Fig. 17. u -cuts at $v=0.25$: (a) magnitude and (b) phase.

IV. CONCLUSION

In this paper, a novel approach based on CZT is proposed to accurately and efficiently compute pattern of general linear or planar antenna arrays. The

corresponding parameters of CZT are derived, making it suitable for antenna array factor computation. Computation processes are also explored and given in this paper. Simulation results prove that it is applicable with high accuracy and efficiency, especially for planar array with equally or unequally spaced elements.

REFERENCES

- [1] C. A. Balanis, *Antenna Theory - Analysis and Design*. 2nd ed., Harper & Row New York, 2005.
- [2] N. Anselmi and L. Poli, "Design of simplified array layouts for preliminary experimental testing and validation of large AESAs," *IEEE Trans. on Antennas Propagation*, vol. 66, no. 12, pp. 6906-6920, Dec. 2018.
- [3] Y. Ma and S. Yang, "Pattern synthesis of 4-D irregular antenna arrays based on maximum-entropy model," *IEEE Trans. on Antennas Propagation*, vol. 67, no. 6, pp. 3048-3057, May 2019.
- [4] B. Zhang and Y. Rahmat-Samii, "Robust optimization with worst case sensitivity analysis applied to array synthesis and antenna designs," *IEEE Trans. on Antennas Propagation*, vol. 66, no. 1, pp. 160-171, Jan. 2018.
- [5] V. V. Bhargava and G. K. Mahanti, "Minimization of side lobe level of scanned linear array antenna with fixed dynamic range ratio utilizing iterative fast Fourier transform," *IEEE Applied Electromagnetic Conf.*, Kolkata, India, Dec. 18-22, 2011.
- [6] L. R. Rabiner and R. W. Schafer, "The chirp z-transform algorithm," *IEEE Trans. Audio and Electroacoustics.*, vol. 17, no. 2, pp. 86-92, June 1969.
- [7] J. A. Draidi and M. A. Khasawneh, "Two-dimensional chirp z-transform and its application to zoom Wigner bispectrum," *IEEE International Symposium on Circuits and Systems*, Atlanta, GA, vol. 2, pp. 540-543, May 12-15, 1996.
- [8] T. G. Stockham, "High speed convolution and correlation," *1966 Spring Joint Computer Conf., AFIPS Proc.*, vol. 28, Washington, D. C.: Spartan, pp. 229-233, 1966.
- [9] C. L. Dolph, "A current distribution for broadside arrays which optimizes the relationship between beamwidth and sidelobe level," *Proc. IRE*, vol. 34, no. 6, pp. 335-348, 1946.
- [10] P. M. Woodward and J. D. Lawson, "The theoretical precision with which an arbitrary radiation-pattern may be obtained from a source of a finite size," *J. IEE*, vol. 95, pt. III, no. 37, pp. 363-370, Sept. 1948.
- [11] C. Lin, A. Qing, and Q. Feng, "Synthesis of unequally spaced antenna arrays by using differential evolution," *IEEE Trans. on Antennas Propagation*, vol. 58, no. 8, pp. 2553-2560, Aug. 2010.



Cheng Zhang was born in Zhongwei, Ning'xia Province, China, in 1988. He received the B.S. degree in Optical Information Science and Technology and the M.Sc. degree in Electronics and Communication Engineering from the University of Electronic Science and Technology of China (UESTC), Chengdu, Sichuan, China, in 2011 and 2014, respectively. Now, he is currently pursuing the Ph.D. degree in Radio Physics at UESTC.



Anyong Qing (S'97–M'00–SM'05) was born in Hu'nan province, China, on May 27, 1972. He received the B.E. degree from Tsinghua University, in 1993, the M.E. degree from Beijing Broadcasting Institute, Beijing, China, in 1995, and the Ph.D. degree from Southwest Jiaotong University in 1997, all in Electromagnetic Theory and Microwave Technology. He was a Postdoctoral Fellow in the Department of Communication Engineering, Shanghai University, Shanghai, China, between September 1997 and June 1998 and a Research Fellow at the School of Electrical and Electronic Engineering, Nanyang Technological University, Singapore from June 1998 to June 2000. He was a Member of Scientific Staff in the Electromagnetic Theory Group at the Department of Electrical Engineering, University of Kassel, Kassel, Germany, from July 2000 to May 2001. He was a Research Scientist at Temasek Laboratories, National University of Singapore, Singapore, from

September 2001 to December 2009 and a Senior Research Scientist from January 2010 to October 2012. He was a Professor with School of Physics, University of Electronic Science and Technology of China, Chengdu, China since November 2012 (part time since December 2017). He is currently chairing Department of Electrical Electronics, Southwest Jiaotong University, Chengdu, China. His research interests include terahertz theory & technology, photo acoustic theory & technology, compressive sensing, natural optimization, computational acoustics & electromagnetics, inverse acoustic & electromagnetic scattering, electromagnetic composite materials, antennas & antenna arrays, millimeter wave & terahertz imaging, and biomedical imaging. He was granted National Young Thousand Talent professorship in September 2011. He is a member of Material Research Society Singapore, and a member of the Chinese Institute of Electronics. He is an Associate Editor of Radio Science since 2017.



Yang Meng received the B.S. degree in Electronic Information Science and Technology from Chongqing University of Arts and Sciences, Chongqing, China in 2014. He is currently pursuing the Ph.D. degree in Radio Physics with University of Electronic Science and Technology of China, Chengdu, China, under the supervision of Professor Anyong Qing. His research interests include the areas of millimeter wave imaging, electromagnetic scattering, and inverse scattering.